III.D.6 Advanced Measurement and Modeling Techniques for Improved SOFC Cathodes

Objectives

- Develop microelectrodes for improved isolation and measurement of the SOFC cathode overpotential (resistance) on cells having a thin electrolyte membrane.
- Develop nonlinear electrochemical impedance spectroscopy (NLEIS) for use in identifying what steps limit SOFC cathode performance.
- Generate a more detailed understanding of the electrochemistry governing SOFC cathodes, facilitating discovery and design of improved cathode materials and microstructures.

Accomplishments

- Developed microelectrode techniques to better isolate the electrochemical response of SOFC cathodes under realistic fabrication and operating conditions.
- Measured the *i-V* characteristics, impedance, and NLEIS of porous and thin-film $La_{1-x}Sr_xCoO_{3-\delta}$ (LSC) electrodes on rare-earth-doped ceria, including 1st, 2nd, and 3rd harmonics.
- Developed *1-D* models for the harmonic response of porous and thin-film LSC electrodes, allowing interpretation of harmonic data.
- Identified *dissociative adsorption* as a critical step in O_2 reduction on electron-rich materials such as LSC, with consequences for new catalyst development.

Introduction

Many promising new cathode materials for solid oxide fuel cells incorporate *mixed conducting ceramics*

Stuart B. Adler (Primary Contact),
Jamie R. Wilson, Shawn L. Huff, and
Yunxiang Lu

University of Washington
Department of Chemical Engineering, Box 351750
Seattle WA 98195-1750
Phone: (206) 543-2131; Fax: (206) 685-3451
E-mail: stuadler@u.washington.edu

DOE Project Manager: Lane Wilson
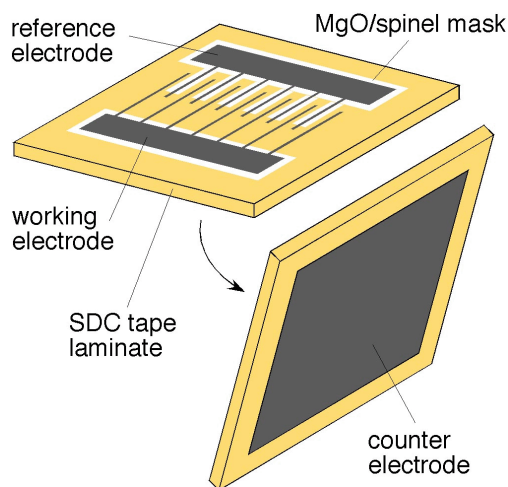Phone: (304) 285-1336
E-mail: Lane.Wilson@netl.doe.gov

(materials which carry both oxygen ions and electrons) in order to substantially enhance oxygen reduction at reduced temperature [1]. For example, $La_{1-x}Sr_xCo_{1-y}Fe_yO_{3-\delta}$ (LSCF) cathodes utilize a significant portion of the electrode material surface, extending the reaction up to 10 microns from the electrode/electrolyte interface [2]. While these electrodes have proven promising in early exploratory research, they are only empirically understood [3], far from optimized [4,5], and can react unfavorably with the electrolyte [6,7]. Significant modification of these materials, or development of new materials, is required to bring this type of electrode to commercial fruition.

In order to address these issues, we believe a new generation of diagnostic tools is required to accelerate screening, fabrication, optimization, and long-term performance evaluation of cathode materials. The role of this project has been twofold. First, we have developed a technique involving microelectrodes (made using standard materials and fabrication techniques) that offers improved accuracy, faster throughput, and broader screening capabilities. Secondly, we have developed an extension of electrochemical impedance spectroscopy (EIS) that involves perturbation and detection of nonlinear electrode response. This technique, called *nonlinear electrochemical impedance spectroscopy* (NLEIS) [8,9], provides much higher resolution in terms of identifying rate-determining steps, separating anode and cathode response, and potentially improved prediction cell performance based on half-cell measurements.

Approach

Figure 1 shows a schematic of the microelectrode cell design we are currently pursuing. The light area on the electrolyte surface is a mask layer that regulates where the working and reference electrodes make contact to the electrolyte. In this way, the ohmic losses are well defined, and confined to a region close to the working electrode (cathode) of experimental interest. Numerical simulations of this arrangement suggest that it provides a high degree of accuracy and frequency isolation. The mask layer is currently fabricated by screenprinting and firing a MgO/spinel mixed powder ink onto a dense (fired) tape of Sm-doped ceria (SDC) electrolyte. The electrodes are subsequently processed onto the cell under the same conditions as any ordinary cell. Electrochemical measurements are then made, and performance normalized to the actual area of the working electrode.

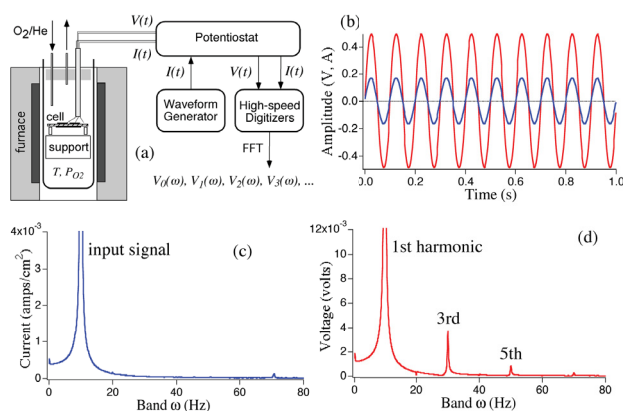**FIGURE 1.** Cell Configuration of a Microelectrode Half-Cell

FIGURE 2. Schematic of NLEIS, as applied to SOFC cathodes. (a) Experimental set-up. (b) Current input and voltage response at 10 Hz for a symmetric cell of $La_{0.6}Sr_{0.4}FeO_{3-d}$ on SDC at 750°C in air. (c) Fourier transform of current signal. (d) Voltage signal.

Figure 2 outlines how we conduct a typical NLEIS experiment. The cell is placed in a controlled atmosphere chamber within a furnace, and interfaced to a potentiostat using spring-loaded gold (Au) current collectors. A sinusoidal current perturbation of variable amplitude is applied to the cell. Voltage and current data are synchronously digitized, and Fourier transformed to obtain frequency domain signals, from which the 1st harmonic (impedance) and higher order harmonics can be readily quantified. This technique has the ability to identify very small nonlinearities (~10^{-3} of the main signal), and naturally filters out non-periodic or asynchronous signals, including small performance drifts or noise. More details regarding the acquisition and processing of NLEIS data are given elsewhere [8].
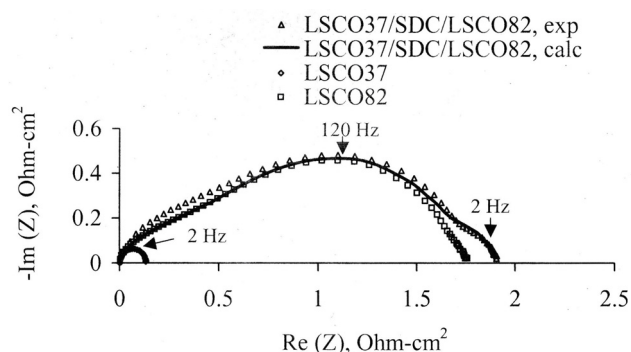

**FIGURE 3.** Impedance of LSC/SDC Cells in Air at 750°C

Results

Microelectrodes. Figure 3 shows the measured impedance of three cells. The first cell consists of a Sm-doped ceria (SDC) electrolyte, coated on one side with a full-sized (1 cm^2) porous $La_{0.3}Sr_{0.7}CoO_{3-\delta}$ (LSC-37) electrode, and on the other with a full-sized porous $La_{0.8}Sr_{0.2}CoO_{3-\delta}$ (LSC-82) electrode. The other two cells are microelectrode half-cells, consisting of LSC-37 and LSC-82 working electrodes, respectively, on SDC. Both half-cells have a 1 cm^2 LSC-82 counterelectrode. With the exception of the mask layer, the microelectrode half-cells were processed identically to the cell with full sized electrodes. Due to differences in composition and processing temperature, the LSC-37 and LSC-82 electrodes have very different characteristics; the impedance magnitude of the LSC-82 electrode is about 10 times larger than the LSC-37 electrode, and it has a characteristic frequency approximately 100 times higher.

As shown in Figure 3, the impedance of the LSC-37/SDC/LSC-82 cell consists of two arcs, which presumably represent contributions of the two electrodes, respectively. In contrast, the microelectrode half-cells show only one arc, which differ from each other in resistance and frequency response. After area normalization, the impedance of the two half-cells were added, yielding a "calculated" impedance spectrum for a LSC-37/SDC/LSC-82 cell, assuming the same ohmic membrane resistance as the actual cell. The data lie nearly on top of each other, which is a testament to both the accuracy and frequency isolation of the microelectrodes, as well as the reproducibility of fabrication in this case.

NLEIS. As shown by Kawada [10], the traditional impedance (EIS) response of a dense thin film LSC electrode can be used to isolate and quantify the oxygen exchange reaction at the surface.

However, other than telling us the P_{O2} dependence of the oxygen exchange rate, there is nothing distinguishing about the EIS signal that reveals anything about the mechanism itself. The EIS response of
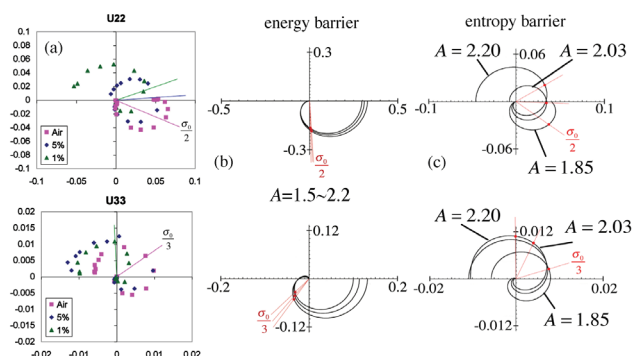
FIGURE 4. (a) 2nd and 3rd harmonic responses U_{22} and U_{33} of a dense thin-film $La_{0.6}Sr_{0.4}CoO_{3-\delta}$ electrode on samaria-doped ceria as a function of P_{O2} at 725°C. The data have been scaled relative to the 1st harmonic. The marked lines are phasors indicating the phase of the data where the frequency is an indicated fraction of the measured characteristic frequency σ_0. (b) and (c) Predicted response based on models discussed in the text.

this type of electrode is almost perfectly semicircular, exhibiting no changes in shape with T or P_{O2}.

In contrast, Figure 4(a) shows Nyquist plots of the 2nd and 3rd harmonic responses, U_{22} and U_{33}, of a dense LSC thin film made by Kawada's group. The size, shape, and phase of the higher harmonics vary strongly over the small range of P_{O2} conditions. The shape changes are specific, including a nullification (change in sign) in the second harmonic at low frequency. The phase of the higher harmonics rotate in a distinct pattern as the P_{O2} is decreased. Figures 4(b) and 4(c) show simulations of the higher harmonics based on two different models for the O_2 exchange reaction. In Figure 4(b), we consider the reaction to be limited by an *energetic* barrier to O_2 dissociation, as is often assumed in the literature. In Figure 4(c), the reaction is limited by the low probability of dissociative adsorption (*entropy barrier*). While both models predict exactly the same EIS response (a semicircle), the first model (energy barrier) is completely inconsistent with the higher harmonic data. Numerous other models that assume various rate-limiting steps (including molecular adsorption, or ion incorporation into the bulk) also fail. Only the model that assumes dissociative adsorption as limiting appears to explain our data. The model is consistent in magnitude, sign, and phase rotation with P_{O2}, and this P_{O2} dependency can be explained quantitatively in terms of the thermodynamic properties of the film.

If our interpretation is correct, it suggests that the strong Arrhenius dependence seen by workers in the exchange rate vs. temperature is not a true activation barrier. Rather, the strong temperature dependence arises from a large negative enthalpy of dissociative adsorption. At higher temperatures more sites on the surface become available, causing an increase in

the dissociative adsorption rate. This result raises the question about whether researchers in this area are barking up the wrong tree. If oxygen reduction is governed by dissociative adsorption, and the adsorption sites are already maximized in terms of concentration, efforts to more easily break the O_2 bond will not help. Useful alternative strategies might include a) increasing the stability of reduced diatomic intermediates at high temperature, thereby increasing their lifetime on the surface, or b) enhancing surface diffusion of oxygen vacancies, thereby decreasing the time between collisions with unstable short-lived diatomic intermediates. In contrast, strategies attempting to decrease the energetic barrier to O_2 dissociation could actually backfire, since any thermodynamic stabilization of monatomic oxygen might lower surface site concentrations.

Conclusions and Future Directions

- Microelectrodes potentially offer an easy, low-cost way to isolate the performance of a particular electrode, while maintaining the composition, microstructure, and processing of that electrode as closely as possible to the real thing.

- NLEIS appears to be a very useful and powerful new technique, which provides higher resolution than traditional linear impedance for distinguishing specific mechanisms governing electrode response.

- Oxygen reduction on mixed conducting perovskite surfaces appears to be limited by site availability for dissociative adsorption rather than scission of the O_2 bond. Developers of new catalysts may wish to consider this in developing new materials strategies.

Special Recognitions & Awards/Patents Issued

FY 2006 Publications/Presentations

1. Wilson, J.R., Schwartz, D.T., and Adler, S.B., *Electrochimica Acta.* **51** (8-9), 1389 (2006).

References

1. Adler, S.B.; Factors governing oxygen reduction in solid oxide fuel cell cathodes, Chemical Reviews 104 (10): 4791-4843, October 2004.

2. Wilson, J.R., Schwartz, D.T., and Adler, S.B., *Electrochimica Acta*. **51**(8-9), 1389 (2006)**.**

3. Wilson, J.R., Schwartz, D.T., Adler, S.B., Sase, M., and Kawada, T., *to be published*.

4. Kawada, T.; Suzuki, J.; Sase, M.; Kaimai, A.; Yashiro, K.; Nigara, Y.; Mizusaki, J.; Kawamura, K.; Yugami, H. Journal of the Electrochemical Society 149, E252-E259 (2002).